

# Use of a Surface-Acoustic-Wave Sensor To Characterize the Reaction of Styrene Vapor with a Square-Planar Organoplatinum Complex

Edward T. Zellers,<sup>\*1</sup> Richard M. White,<sup>2</sup> and Stephen M. Rappaport<sup>3</sup>

Department of Environmental and Industrial Health, School of Public Health, University of Michigan, Ann Arbor, Michigan 48109-2029, Department of Electrical Engineering and Computer Sciences and Berkeley Sensor and Actuator Center, University of California, Berkeley, California 94720, and Department of Biomedical and Environmental Health Sciences, School of Public Health, University of California, Berkeley, California 94720

A coated surface-acoustic-wave (SAW) sensor is used to probe the reaction of styrene vapor with the square-planar platinum-ethylene  $\pi$ -complex, *trans*-PtCl<sub>2</sub>(ethylene)(pyridine). A dual-SAW delay-line oscillator configuration is employed: one oscillator is coated with a solvent-cast film of the solid platinum-ethylene complex dispersed in a poly(isobutylene) matrix, and the second oscillator is coated only with polymer. Absorbed styrene vapor displaces ethylene to form the stable styrene-substituted complex, *trans*-PtCl<sub>2</sub>(styrene)(pyridine), causing a decrease in the oscillator frequency from the increase of mass on the surface of the sensor. For short-term exposures, there is a linear relationship between the logarithm of the rate of frequency change and the logarithm of the styrene vapor concentration, consistent with a power-law kinetic model for the heterogeneous trapping reaction. Deviation from this relationship above 300 ppm at 25 °C is attributed to the onset of multilayer adsorption of styrene at the surface of the trapping reagent. The sensor response exhibits an Arrhenius temperature dependence permitting estimation of the thermal activation energy for the olefin-substitution reaction. Calculated detection limits of 3 and 0.6 ppm of styrene vapor are achieved for operation at 25 and 40 °C, respectively.

## INTRODUCTION

Research on coated surface-acoustic-wave (SAW) chemical sensors has focused primarily on the detection of gas-phase analytes. By variation of the nature of the surface coating, SAW sensors have been developed for a number of organic and inorganic gases and vapors (1-10). Like other ultrasonic-oscillator sensors, such as the bulk-acoustic-wave (BAW) (11) and Lamb-wave (12) sensors, the coated-SAW sensor responds to changes in the physical properties of the coating on the sensor surface. Advantage has been taken of this feature not only for gas and vapor monitoring applications but also for characterizing the physicochemical properties of the coating materials. For example, coated-SAW sensors have been used to examine the thermodynamics of water-vapor sorption in hygroscopic polymers (13), thermally induced phase transitions in organic polymers (14, 15), vapor diffusion coefficients in thin films of polyimide, and surface areas of microporous inorganic sol-gel films (16). Partition coefficients of various organic vapors into an oligomeric stationary phase

deposited on the surface of a SAW sensor have also been reported (17).

In the course of our investigations into reagent-based SAW-sensor coatings for olefin gases and vapors, we have found that the sensor responses can be used to obtain fundamental information about the nature of the heterogeneous trapping reaction between the coating and the analyte vapor. The sensor coating used here consists of a mixture of the solid reagent *trans*-PtCl<sub>2</sub>(ethylene)(pyridine) and the amorphous rubbery polymer poly(isobutylene) (PIB). Reaction between this reagent and absorbed styrene vapor results in a continuous concentration-dependent change in the output frequency of the sensor.

The trapping reagent is one member of a class of square-planar platinum-olefin  $\pi$ -complexes of the general formula, *trans*-PtCl<sub>2</sub>(olefin)(amine), whose ligand-substitution behavior has been studied extensively (18-23). In the case of nucleophilic attack by olefins, reversible substitution of the initially bound olefin occurs with retention of the spatial configuration of the ligands in the olefin-substituted product. For complexes where the amine is pyridine or a substituted pyridine, olefin-substitution reactions proceed under mild conditions via an associative bimolecular transition state (21, 22).

In this paper, we show how the SAW sensor can be used to characterize the kinetics and thermodynamics of the vapor-coating interactions. The companion paper that follows describes the performance of the sensor as an environmental monitor for styrene and examines the effects of humidity and other relevant industrial co-contaminants on the response to styrene, as well as the regeneration of the trapping reagent.

**Sensor Design and Operation.** Since details of the design and operation of the coated-SAW chemical sensor have been described elsewhere (24), only the salient operating features are given here. The SAW delay-line oscillator consists of a polished piezoelectric substrate having a pair of evaporated-metal interdigital transducers (IDT) deposited on its surface and connected via an external feedback amplifier. Application of a voltage to the input IDT results in oscillation at a frequency whose value is determined by the velocity of the wave in the substrate, the distance between the IDTs, and the spacings of the IDT electrodes.

Equation 1 gives an approximate expression for the change of the oscillator frequency upon deposition of a thin, nonconducting, low-modulus, isotropic coating film (24, 25)

$$\Delta f = (k_1 + k_2)f_0^2h\rho = (k_1 + k_2)f_0^2m/a \quad (1)$$

where  $\Delta f$  is the change of frequency,  $k_1$  and  $k_2$  are negative substrate-dependent constants of the order  $10^{-8}$  (m<sup>2</sup>/(kg s)),  $f_0$  is the resonant frequency (Hz),  $\rho$  is the density of the coating film (kg/m<sup>3</sup>),  $h$  is the coating film thickness (m), and  $m/a$  is the mass per unit area of the coating film (kg/m<sup>2</sup>). This relationship can be used to estimate the initial mass or

<sup>1</sup> Department of Environmental and Industrial Health, School of Public Health, University of Michigan.

<sup>2</sup> Department of Electrical Engineering and Computer Sciences and Berkeley Sensor and Actuator Center, University of California.

<sup>3</sup> Department of Biomedical and Environmental Health Sciences, School of Public Health, University of California.

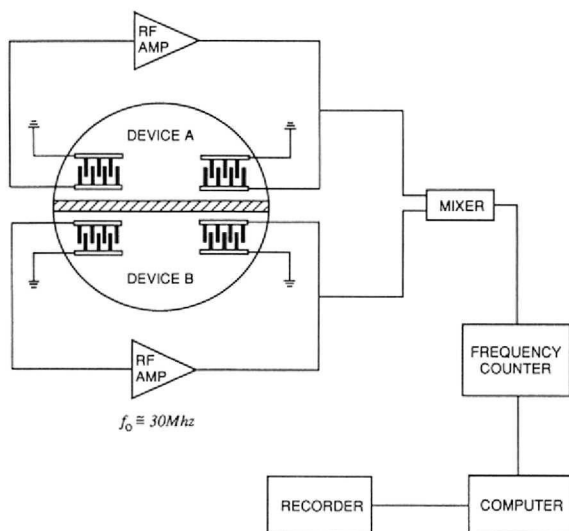


Figure 1. Schematic diagram of dual-SAW sensor and associated measurement equipment.

thickness of the coating film deposited on the oscillator and to monitor subsequent changes of the coating mass due to interactions with a gas or vapor. For a 30-MHz oscillator on ST-quartz with an active area of  $1.5 \text{ cm}^2$ , such as that used here, eq 1 predicts a change of about 840 Hz for every microgram change of surface mass.

## EXPERIMENTAL SECTION

**Reagent Synthesis.** All starting materials and solvents were of reagent grade or higher purity and were used without further purification. Melting points were determined with a Mettler FP-52 hot stage with an optical microscope. Elemental analyses were performed by Galbraith Laboratories, Knoxville, TN. Infrared spectra were recorded on a Perkin-Elmer 775B IR spectrophotometer.

The trapping reagent, *trans*-PtCl<sub>2</sub>(ethylene)(pyridine), was synthesized by a known procedure (21) involving the addition of pyridine (Aldrich) to an aqueous solution of Zeise's salt, KPtCl<sub>3</sub>(ethylene) (Alfa). The solid precipitate was recrystallized from methylene chloride/petroleum ether, mp 112 °C (dec). Anal. Calcd: C, 22.5; H, 2.4; N, 3.7. Found: C, 22.5; H, 2.5; N, 3.7. The corresponding styrene-substituted compound was synthesized by adding a 4-fold excess of styrene (Aldrich) to a methylene chloride solution of PtCl<sub>2</sub>(ethylene)(pyridine) followed by refluxing for 10 min (19). The solid styrene complex was isolated in pure form by the addition excess petroleum ether (mp 124 °C). Both of the complexes are yellow crystalline solids that are soluble in polar organic solvents such as methylene chloride, chloroform, acetone, and toluene.

**Apparatus.** The sensor and associated measurement equipment are shown schematically in Figure 1. Two matched 30-MHz SAW devices were fabricated on a 2-in. ST-quartz wafer (Valpey-Fischer). Each IDT consisted of 50 pairs of evaporated Au/Cr electrodes (2600 Å thick) having equal widths and spaces of 25  $\mu\text{m}$  and an acoustic aperture (i.e., the overlap length of the electrodes which defines the width of the acoustic wave) of 6000  $\mu\text{m}$ . The distance between the IDT centers was approximately 2 cm, resulting in an active area of  $1.5 \text{ cm}^2$  for each device. Variable series inductors were used as tuning elements to cancel the reactive (i.e., capacitive) component of the impedance in each IDT. Two cascaded LM733 amplifiers provided the gain necessary to maintain oscillations in each device. The signals from the oscillators were passed through a mixer and low-pass filter (LPF) to obtain the difference frequency, which was monitored with a digital frequency counter (Hewlett-Packard 5384A) and logged on a personal computer (Commodore 64 or Hewlett-Packard Vectra) via an IEEE-488 interface. Frequency measurements were collected every 6 s with a resolution of 1 Hz.

The sensor was mounted in a cylindrical stainless steel chamber having an internal volume of 0.24 L and equipped with gas inlet and outlet ports. Electrical connections were made with coaxial

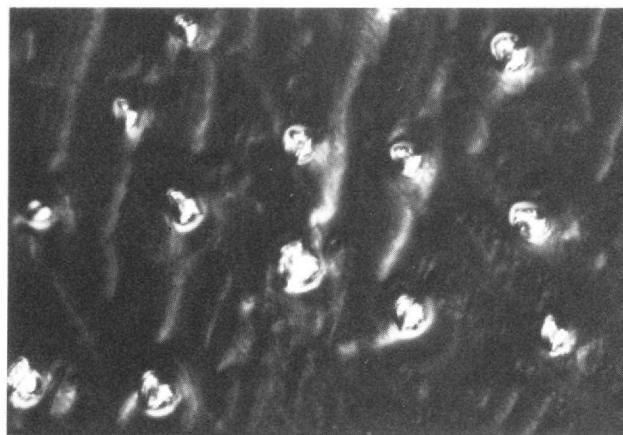


Figure 2. Photomicrograph (500X) of the *trans*-PtCl<sub>2</sub>(ethylene)(pyridine)/PIB sensor coating.

(BNC) connectors through tapped fittings in the floor of the chamber. Heating tape wrapped around the exposure chamber and the immediate foreline was used to control the chamber temperature, and a thermocouple was used to monitor the temperature at the surface of the sensor. Dynamic (i.e., continuous flow) test atmospheres of the solvent vapors were generated by passing nitrogen gas through a fritted-glass bubbler containing the liquid solvent and then into a metered dilution-air stream. After passing through a length of tubing to ensure adequate mixing, the air stream was divided, with a portion being directed to the exposure chamber and the remainder passing through an infrared gas analyzer (Foxboro, MIRAN 1A) used for verification of solvent vapor concentrations. A calibrated rotameter was used to maintain a flow of 8 L/min through the exposure chamber, corresponding to a theoretical mixing time of 8 s (26). Dilution-air flow, temperature, and relative humidity (RH) were controlled with a Miller-Nelson Research HCS 301 control unit.

**Coating-Film Deposition.** We found that combining the solid complex with the amorphous, rubbery polymer poly(isobutylene) (PIB,  $T_g = -65$  °C, Scientific Polymer Products) resulted in more uniform coating films and more consistent results than those obtained by using the solid complex alone. Several coating deposition techniques were examined including sublimation (of the platinum-ethylene complex), spraying, dipping, painting, and solvent casting. Solvent casting gave the best uniformity and reproducibility of films as judged by visual and microscopic inspection. The resulting films consisted of roughly cubic crystals of the complex dispersed randomly throughout the polymer film (Figure 2). Solutions containing 6 mg/mL of each component in 3/1 toluene-hexane were applied to the sensor surface with a micropipet, and the mass deposited was estimated by using the net frequency shift of the oscillator upon evaporation of the casting solvent (via eq 1).

From the estimate of deposited mass, nominal coating thicknesses could be calculated by using the mean of the densities for each of the components (918 and 2400 kg/m<sup>3</sup> for the PIB and the platinum-ethylene complex, respectively). Thicknesses ranging from about 1 to 2.5  $\mu\text{m}$ , corresponding to coating masses of 20–590  $\mu\text{g}$  (120–295  $\mu\text{g}$  of PtCl<sub>2</sub>(ethylene)(pyridine)), could be obtained by multiple solvent castings. For the experiments described below, coating thicknesses typically ranged from 1.8 to 2  $\mu\text{m}$ . The reference device was coated with an equivalent thickness of PIB so that measuring the difference frequency would cancel the response due to sorption and desorption of vapors by the polymer on the sensing oscillator.

## VAPOR-COATING INTERACTIONS

The principal interactions occurring between styrene and the *trans*-PtCl<sub>2</sub>(ethylene)(pyridine)/PIB sensor coating film are depicted in Figure 3. Upon exposure to a given styrene-vapor concentration, the coating film (on each oscillator) sorbs styrene to an extent determined by the equilibrium air/film partition coefficient,  $K$ . The sorbed styrene then reacts with the platinum-ethylene complex at a rate determined by the effective styrene concentration at the surface

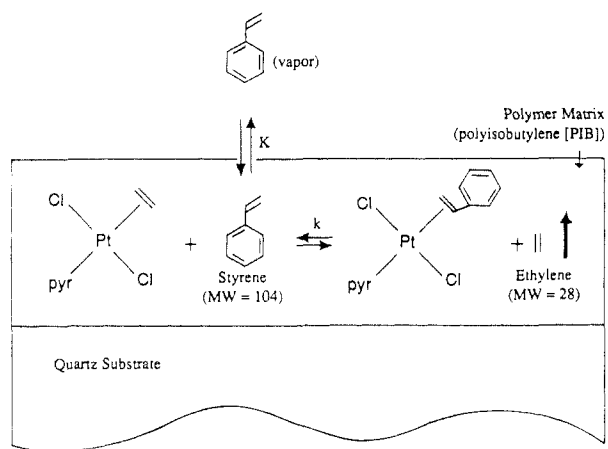


Figure 3. Interactions between the sensor coating and styrene vapor.

of the solid and the rate constant for the reaction,  $k$ . The reaction results in the formation of the corresponding platinum-styrene complex, *trans*-PtCl<sub>2</sub>(styrene)(pyridine), and evolution of ethylene gas. While the olefin substitution reaction is reversible, the combination of an excess of styrene and the release of volatile ethylene from the film drives the equilibrium to the right.

As the styrene reacts with the complex, the equilibrium concentration of free styrene in the polymer decreases proportionally, causing more styrene to be sorbed by the polymer. Since styrene (MW = 104) is heavier than ethylene (MW = 28), there is a continual increase of surface mass and, consequently, a continual reduction of the frequency of the SAW oscillator. By measurement of the difference frequency of the two oscillators, the initial response (i.e., mass increase) due to polymer sorption of styrene (and other solvent vapors), which can be several hundred hertz in magnitude, is effectively cancelled and the measured frequency shift is due only to the chemical reaction.

Since the sensor frequency shift is directly proportional to changes of coating mass, the rate of change of frequency should be directly proportional to the rate of reaction of styrene vapor with the platinum-ethylene complex. Further, since there is 1:1 stoichiometry of all reactants and products, the steady-state reaction rate can be given in any of the following equivalent forms

$$\text{rate} = -dN_{\text{Pt-eth}}/dt = -dN_{\text{sty}}/dt = dN_{\text{Pt-sty}}/dt = dN_{\text{eth}}/dt \quad (2)$$

where  $N$  is the number of moles and the subscripts refer, respectively, to the platinum-ethylene complex, styrene, the platinum-styrene complex, and ethylene.

The rate of frequency change resulting from a given rate of mass change on the surface of the sensor can be expressed as

$$df/dt = C dm/dt \quad (3)$$

where  $C = (k_1 + k_2 f_0)/a$  from eq 1.

At steady state, there is a continual change of mass at the device surface as styrene replaces ethylene in the complex. Thus, the rate of frequency change can be written as

$$df/dt = C(dm_{\text{sty}}/dt - dm_{\text{eth}}/dt) = C(MW_{\text{sty}} dN_{\text{sty}} - MW_{\text{eth}} dN_{\text{eth}})/dt \quad (4)$$

where  $m_i$  and  $MW_i$  refer, respectively, to the mass and the molecular weight of the  $i$ th species.

From the equivalent rate expressions in eq 2, we have  $dN_{\text{eth}}/dt = -dN_{\text{sty}}/dt = -dN_{\text{Pt-eth}}/dt$ . Thus

$$df/dt = -C(MW_{\text{sty}} - MW_{\text{eth}})dN_{\text{sty}}/dt = C'dN_{\text{Pt-eth}}/dt \quad (5)$$

which shows the proportionality between the rate of the trapping reaction and the rate of frequency change of the sensor.

Provided that the rate-limiting step is the first-order reaction with styrene, the rate of frequency change depends on the instantaneous styrene-air concentration. The net frequency shift measured after exposure is also related to the integrated exposure level (i.e., concentration  $\times$  time); however, the primary focus of the discussions that follow is on the use of the sensor output to probe the dynamics of the trapping reaction.

## RESULTS AND DISCUSSION

**Verification of Reaction Products.** IR spectrophotometry was used to document formation of the styrene-substituted product. A squalane mull of PtCl<sub>2</sub>(ethylene)(pyridine) was applied to a KBr plate and exposed to about 100 ppm of styrene over several hours at room temperature. The sample was periodically removed from the exposure chamber to record the IR spectrum and compare it to the spectra of authentic samples of each complex. The gradual emergence of absorbances at 1000, 580, and 540 cm<sup>-1</sup> (corresponding to the platinum-styrene complex) along with a concomitant reduction in the strength of absorbance at 1035 and 960 cm<sup>-1</sup> (corresponding to the platinum-ethylene complex) confirmed that the reaction was proceeding. Complete conversion of the sample was indicated after several hours of exposure.

**Polymer Sorption.** Initial tests were performed to characterize the response to styrene of a single SAW oscillator coated only with PIB ( $\sim 2 \mu\text{m}$ ). Exposure to a given styrene concentration resulted in a rapid negative frequency shift followed by reestablishment of a stable (lower) frequency corresponding to the equilibrium mass of styrene sorbed by the polymer. Upon removal of styrene from the atmosphere the frequency recovered to the preexposure value. The initial response of the sensor upon introduction or removal of styrene was very rapid, with large frequency shifts being observed within 6 s. The time required to reach the equilibrium frequency shift (response or recovery) ranged from about 15 to 90 s for styrene vapor concentrations of 5 to 700 ppm, respectively.

Exposure of the PIB-coated oscillator to styrene concentrations from 5 to 700 ppm at temperatures of 15, 25, 32, and 40 °C yielded a series of linear sorption isotherms, indicating that the concentration of styrene in the polymer is proportional to its air concentration. As expected, the frequency shift for a given styrene concentration decreased with increasing temperature. Since the response of the sensor is proportional to deposited mass, the ratio of the mass of styrene sorbed to the mass of polymer on the device is equal to the ratio of the frequency shifts due to these quantities (17). The slope of the isotherm at each temperature is therefore proportional to the air/polymer partition coefficient. With this relationship, an Arrhenius plot of the data yields a value of -9.9 kcal/mol for the heat sorption ( $\Delta H_s$ ), which is considered typical of vapor sorption in organic polymers (27).

**Sensor Response Curves.** A plot of the rate of frequency change versus styrene concentration for the *trans*-PtCl<sub>2</sub>(ethylene)(pyridine)/PIB-coated sensor at 25 °C is shown in Figure 4a. Each point represents the mean response for exposures of 10–20-min duration at each concentration. The time required to establish a steady-state rate of frequency ranged from about 30 to 180 s for styrene concentrations from 5 to 700 ppm, respectively.

The response to styrene increases over the entire concentration range. Up to 300 ppm there is a continual decrease in sensitivity (Hz/(ppm min)) with increasing concentration in accordance with the heterogeneous nature of the reaction which involves only a limited number of reactive surface sites

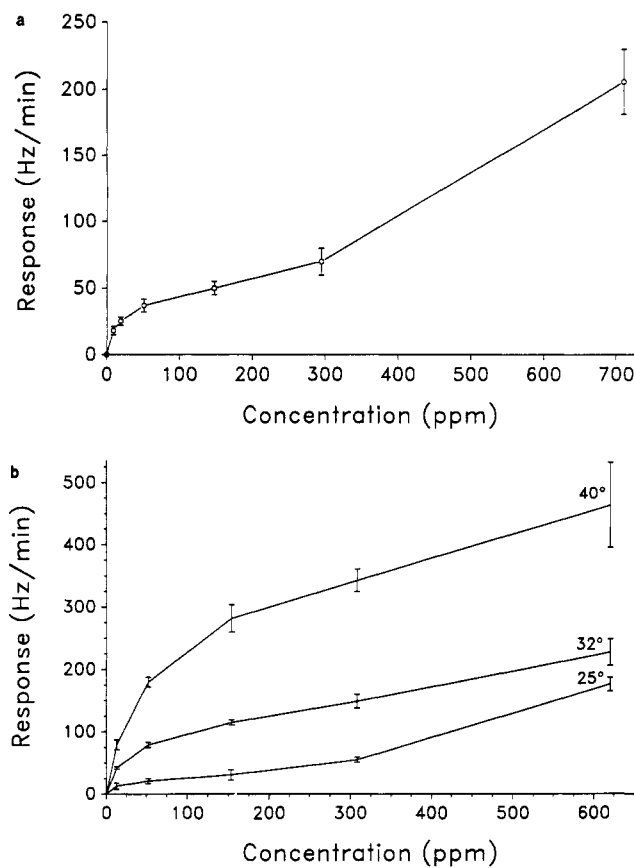


**Figure 4.** (a) Plot of the rate of frequency change (response) versus styrene concentration for operation at 25 °C and 50% relative humidity (RH). (b) Plot of the rate of frequency change (response) versus styrene concentration for operation at 25 °C (lower curve), 32 °C (middle curve), and 40 °C (upper curve) (5% RH). Each point represents the mean response measured for 10–15 min at each concentration.

on the trapping agent. Above 300 ppm, the sensitivity increases slightly, giving rise to the inflection point seen in Figure 4a. In contrast, responses at 32 and 40 °C are monotonic over the entire concentration range and the sensitivity steadily decreases with increasing concentration, as shown in Figure 4b. The increase in sensitivity observed for the higher concentrations at 25 °C can be explained in terms of the vapor–solid reaction kinetics as discussed in the next section.

The shapes of the response curves shown in Figure 4 are highly reproducible. Variations of up to 30% in the sensor response value for a given styrene concentration have been observed between different coatings, which is attributed to differences in both the mass of coating deposited and the surface area of the solid trapping reagent. However, with careful solution preparation and deposition, we have achieved responses differing by less than 6% for replicate coatings within the concentration range of 5–600 ppm for operation at both 25 and 40 °C.

Long-term aging effects have not been examined, although both the platinum–ethylene complex and the platinum–styrene complex solids were stored in capped vials exposed to air for over 3 months with no signs of decomposition. For a number of exposure experiments, the same coating was used repeatedly over the course of several days with no change in response.

**Comparison with Theoretical Gas–Solid Reaction Models.** Since the rate of frequency change is proportional to the rate of reaction of styrene with the platinum–ethylene complex, it is possible to compare the sensor response to theoretical models of gas–solid reactions. For the short-term

**Table I. Linear-Regression Correlation Coefficients ( $r^2$ ) and Ranges of Error Obtained by Fitting Experimental Data from Figure 4b to the LH and Power-Law Kinetic Models<sup>a,b</sup>**

temp, °C	LH model		power-law model	
	$r^2$	% error	$r^2$	% error
25	0.195 (0.832)	— 10–56	0.869 (0.961)	12–47 6–15
32	0.929	7–46	0.993	0–7
40	0.978	4–29	0.984	4–11

<sup>a</sup> Error values were calculated as  $(\text{observed} - \text{predicted})/\text{predicted} \times 100$  using predicted sensor response values obtained from the linear regression model at each temperature. <sup>b</sup> Values in parentheses are for a styrene concentration range of ~10–300 ppm. All other values are for a styrene concentration range of ~10–620 ppm.

exposures considered here it is assumed that the surface area of the solid particle does not change significantly over the course of reaction and the reaction can be considered catalytic. Furthermore, it is assumed that the rate-limiting step of the overall vapor-coating interaction is the reaction at the solid surface.

The Langmuir–Hinshelwood (LH) and power-law models have been used successfully in describing the kinetics of a broad range of gas–solid reaction systems (28, 29). The LH model assumes that gas adsorption follows a Langmuir isotherm and the power-law model assumes a Freundlich adsorption isotherm. Both models assume that the surface reaction is first order with respect to the reactant gas (styrene, in this case) and that the surface coverage asymptotically approaches a monolayer with increasing gas concentration.

The LH expression for the reversible gas/solid reaction considered here is (28)

$$r_{Pt} = (kK_{sty}p_{sty} - p_{eth}/K_e)/(1 + K_{sty}p_{sty} + K_{eth}p_{eth}) \quad (6)$$

where  $r_{Pt}$  is the rate of reaction of the platinum–ethylene complex,  $k$  is the reaction rate constant,  $K_{sty}$  and  $K_{eth}$  are the equilibrium adsorption constants for styrene and ethylene, respectively,  $p_{sty}$  and  $p_{eth}$  are their partial pressures, and  $K_e$  is the equilibrium constant for the overall reaction. For our system the partial pressure of ethylene is very small compared to the partial pressure of styrene, so that eq 6 can be reduced to

$$r_{Pt} = kK_{sty}p_{sty}/(1 + K_{sty}p_{sty}) \quad (7)$$

Rearranging eq 7 into the following form allows comparison of the data with the model using linear regression analysis

$$p_{sty}/r_{Pt} = 1/kK_{sty} + p_{sty}/k \quad (8)$$

Since  $p_{sty}$  is proportional to the styrene vapor concentration in ppm ( $ppm_{sty}$ ) and  $r_{Pt}$  is proportional to the sensor response, plotting  $ppm_{sty}$  versus  $ppm_{sty}/r_{Pt}$  should yield a straight line (note: the concentration of styrene in the polymer phase of the coating is also proportional to the styrene vapor concentration, as discussed above).

The power-law kinetic expression for a reaction that is first order in styrene is (29)

$$r_{Pt} = Fp_{sty}^{1/n} \quad (9)$$

where  $F$  is a combined reaction-rate/adsorption constant and  $n$  is a constant  $>1$ . Adherence to this model is indicated if there is a linear relationship between the logarithm of the rate (sensor response) and the logarithm of  $p_{sty}$  ( $ppm_{sty}$ ).

Table I presents linear-regression correlation coefficients ( $r^2$ ) obtained from fitting the data shown in Figure 4b to each

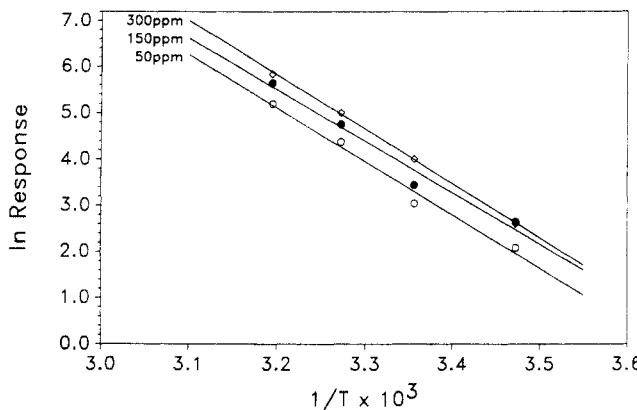


Figure 5. Arrhenius plot of the sensor response at the indicated concentrations for temperatures ranging from 15 to 40 °C.

of the rate models (i.e., eqs 7 and 9). Also presented in Table I are the ranges of error resulting from using the models to predict the sensor response for a given styrene concentration. At 25 °C, the correlation with the LH model is rather poor ( $r^2 = 0.195$ ), reflecting the sensitivity of the model to the assumption of a Langmuir adsorption isotherm. The correlation with the power-law model is much better ( $r^2 = 0.869$ ), but rather large errors are still encountered between the observed and expected values (percent error = 12–47%). Restricting consideration to concentrations  $\leq 300$  ppm (values in parentheses in Table I) improves the fit of the data to both models. At the higher temperatures the correlations with both models are quite good over the entire concentration range examined (note: it is not unusual to find, as we do here, similar correlations with both models since they predict curves of similar shape (30)). Overall, the data appear to fit the power-law model better than the LH model. Errors of less than 15% are obtained by using the power-law model to predict the sensor responses, with the exception of high concentrations measured at 25 °C.

Both of the models predict that the reaction rate should increase with increasing gas partial pressure, asymptotically approaching a limiting value as the surface coverage approaches a monolayer. The deviation from this behavior observed above 300 ppm at 25 °C is most likely due to the onset of multilayer styrene adsorption at the reagent surface. The lower activation energy required for reaction with styrene molecules in these subsequent layers would explain the higher-than-expected reaction rate. That we do not see this behavior at higher temperatures is consistent with this explanation since multilayer adsorption would be expected to diminish at higher temperatures for a given styrene concentration. Slower diffusion of styrene within the solid at 25 °C may also be affecting the overall reaction rate and contributing to the lack of fit to the models.

**Activation Energy.** For a given styrene concentration, there is a positive-exponential (Arrhenius) dependence of the response on temperature. Figure 5 shows Arrhenius plots for exposure to 50, 150, and 300 ppm of styrene at temperatures ranging from 15 to 40 °C. The curves are all linear (linear-regression  $r^2$  values range from 0.973 to 0.999) and from their slopes a mean thermal activation energy of  $22.8 \pm 0.3$  kcal/mol is obtained. Studies of similar reactions in solution, where the olefins involved were substituted butenes, yielded values of 13–20 kcal/mol (22). While the agreement with these previous data is quite good, the slightly higher value measured for our system may reflect the positive temperature dependence of diffusion of the styrene (or ethylene) in the solid trapping agent. Apparently, transport of the styrene through the polymer is fast relative to the chemical reaction since the response (reaction rate) increases with increasing temperature

even though equilibrium polymer sorption decreases.

**Limit of Detection.** The lower detection limit for the sensor was determined by extrapolation from the responses measured at 5 ppm. We define the detection limit as  $3\sigma/\text{sensitivity}$ , where  $\sigma$  is the standard deviation of the noise (31). Using the measured sensitivity of  $4 \text{ Hz}/(\text{ppm min})$  at 5 ppm and a value for  $\sigma$  of  $4 \text{ Hz}/\text{min}$  (measured before and after exposure), a detection limit of 3 ppm is obtained for operation at 25 °C. This is considered a conservative (high) estimate since the slope of the response curve is probably slightly higher than that measured at 5 ppm. If the data collected at 40 °C are used instead, a detection limit of 0.6 ppm is obtained.

## CONCLUSIONS

We have shown that the coated-SAW sensor can serve as a useful probe of vapor-solid reactions. The output from the sensor has been used to calculate the heat of sorption of styrene in poly(isobutylene) and the activation energy for the reaction of styrene vapor with *trans*-PtCl<sub>2</sub>(ethylene)(pyridine). The direct relationship between the sensor response and the rate of the trapping reaction also enables a comparison of sensor response data with theoretical kinetic models. For the heterogeneous olefin-substitution reaction studied here, a better correlation was found with a power-law kinetic model than a Langmuir–Hinshelwood model as indicated by the linear relationship between the logarithm of the sensor response and the logarithm of the styrene vapor concentration for operation above room temperature. Deviation from this relationship observed at 25 °C for styrene concentrations exceeding 300 ppm is attributable to the onset of multilayer adsorption of styrene at the surface of the solid trapping agent.

In addition to characterizing the vapor-coating interactions, direct measurement of styrene vapor from 5 to 700 ppm has been demonstrated. The calculated detection limits of 3 ppm (25 °C) and 0.6 ppm (40 °C) are quite low considering the modest operating frequency of the sensor (30 MHz). Further improvements in sensitivity would be expected with SAW devices operating at higher frequencies. The strong temperature dependence observed underscores the need for careful thermostating of the sensor during operation. At the same time, this factor provides a means for controlling the reaction rate and the sensitivity to a given styrene vapor concentration.

## ACKNOWLEDGMENT

The authors wish to thank Dr. Andrew Waterhouse for valuable discussions during the early stages of this work and Dr. Juan Goicolea for his assistance during the electrical characterization of the sensor.

## LITERATURE CITED

- 1) Snow, A.; Wohltjen, H. *Anal. Chem.* 1984, 56, 1411.
- 2) Venema, A.; Nieukoop, E.; Vellekoop, M. J.; Ghijssen, W. J.; Barandz, A. W.; Nieuwenhuizen, M. S. *IEEE Trans. Ultrason., Ferroelec., Freq. Control* 1987, 34, 149.
- 3) Nieuwenhuizen, M. S.; Nederlof, A. J.; Barandz, A. W. *Anal. Chem.* 1988, 60, 230.
- 4) D'Amico, A.; Palma, A.; Verona, E. *Sens. Actuators* 1982/83, 3, 31.
- 5) Veltelino, J. F.; Lade, R.; Falconer, R. S. *IEEE Trans. Ultrason., Ferroelec., Freq. Control* 1987, 34, 157.
- 6) Bryant, A.; Lee, D. L.; Veltelino, J. F. *IEEE Ultrason. Symp. Proc.* 1981, 171.
- 7) Wohltjen, H.; Snow, A. W.; Barger, W. R.; Ballantine, D. S., Jr. *IEEE Trans. Ultrason., Ferroelec., Freq. Control* 1987, 34, 172.
- 8) Ballantine, D. S., Jr.; Rose, S. L.; Grate, J. W.; Wohltjen, H. *Anal. Chem.* 1986, 58, 3058.
- 9) Rose-Pehrsson, S. L.; Grate, J. W.; Ballantine, D. S., Jr.; Jurs, P. C. *Anal. Chem.* 1988, 60, 2801.
- 10) Zellers, E. T. In *Chemical Sensors and Microinstrumentation*; Murray, R. W., Ed.; ACS Symposium Series 403; American Chemical Society: Washington, DC, 1989; pp 176–190.
- 11) Alder, J. F.; McCallum, J. J. *Analyst* 1983, 108, 1169.
- 12) Zellers, E. T.; White, R. M.; Wenzel, S. W. *Sens. Actuators* 1988, 14, 35.
- 13) Brace, J. G.; SanFelippo, T. S.; Joshi, S. G. *IEEE Solid-State Sensors Workshop Technical Digest* 1986, 60.
- 14) Wohltjen, H.; Derry, R. E. *Anal. Chem.* 1979, 51, 1458.
- 15) Ballantine, D. S., Jr.; Wohltjen, H. In *Chemical Sensors and Microinstrumentation*; Murray, R. W., Ed.; ACS Symposium Series 403; Am-

erican Chemical Society: Washington, DC, 1989; pp 222-236.

(16) Frye, G. C.; Martin, S. J.; Ricco, A. J.; Brinker, C. J. In *Chemical Sensors and Microinstrumentation*; Murray, R. W., Ed.; ACS Symposium Series 403; American Chemical Society: Washington, DC, 1989; pp 208-221.

(17) Grate, J. W.; Snow, A.; Ballantine, D. S., Jr.; Wohtjen, H.; Abraham, M. H.; McGill, A.; Sasson, P. *Anal. Chem.* 1988, 60, 869.

(18) Herberhold, M. *Metal π-Complexes*; Elsevier: Amsterdam, 1974; Vol. 1, Pts. 1 and 2.

(19) Meester, M. A.; van Dam, H.; Stuifkens, D. J.; Oskam, A. *Inorg. Chim. Acta* 1978, 20, 155.

(20) Meester, M. A.; Stuifkens, D. J.; Vrlese, K. *Inorg. Chim. Acta* 1978, 16, 191.

(21) Orchin, M.; Schmidt, P. J. *Inorg. Chim. Acta. Rev.* 1968, 123.

(22) Miya, S.; Kashiwabara, K.; Saito, K. *Inorg. Chem.* 1980, 19, 98.

(23) Langford, C. H.; Gray, H. B. *Ligand Substitution Processes*; W. A. Benjamin: New York, 1965; Chapter 2.

(24) Wohtjen, H. *Sens. Actuators* 1984, 5, 307.

(25) Auld, B. A. *Acoustic Fields and Waves in Solids*; Wiley and Sons: New York, 1973; Vol. 2.

(26) Nelson, G. O. *Controlled Test Atmospheres*; Ann Arbor Press: Ann Arbor, MI, 1976.

(27) Giddings, J. C. In *Chromatography*, 2nd ed.; Heftmann, E., Ed.; Reinhold: New York, 1967; Chapter 3.

(28) Doraiswamy, L. K.; Sharma, M. M. *Heterogeneous Reactions: Analysis, Examples, and Reactor Design*; Wiley-Interscience: New York, 1984; Vol. 1, Chapter 2.

(29) Chaudari, R. V.; Ramachandran, P. A. *AIChE J.* 1980, 26, 177.

(30) Hayward, D. M.; Crowell, A. D. *Chemisorption*; 2nd ed.; Butterworths: London, 1964; Chapter 1.

(31) Carey, W. P.; Kowalski, B. R. *Anal. Chem.* 1986, 58, 3077-3084.

RECEIVED for review November 8, 1989. Accepted March 8, 1990. This work was supported in part by a donation from Dow Chemical U.S.A., by Training Grant T15-OHO-7205-04 and Research Grant 1-RO1-2663-01 from the National Institute for Occupational Safety and Health of the Centers for Disease Control, by the Northern California Occupational Health Center, and by the University of Michigan School of Public Health.

## Selective Real-Time Measurement of Styrene Vapor Using a Surface-Acoustic-Wave Sensor with a Regenerable Organoplatinum Coating

Edward T. Zellers,<sup>\*1</sup> Noralynn Hassold,<sup>1</sup> Richard M. White,<sup>2</sup> and Stephen M. Rappaport<sup>3</sup>

Department of Environmental and Industrial Health, School of Public Health, University of Michigan, Ann Arbor, Michigan 48109-2029, Department of Electrical Engineering and Computer Sciences and Berkeley Sensor and Actuator Center, University of California, Berkeley, California 94720, and Department of Biomedical and Environmental Health Sciences, School of Public Health, University of California, Berkeley, California 94720

The performance of a coated surface-acoustic-wave (SAW) sensor for monitoring styrene vapor is investigated. The effects of several organic co-contaminants and atmospheric humidity are described, and regeneration of the sensor coating is demonstrated. The dual-SAW delay-line oscillator employs a reagent coating of *trans*-PtCl<sub>2</sub>(ethylene)(pyridine) to trap styrene via ethylene substitution. The rate of change of the sensor frequency is used to provide real-time measurement of styrene vapor concentrations. No effect on the response to styrene is observed upon simultaneous exposure to each of several olefin and non-olefin solvent vapors used with styrene in industrial processes. Butadiene, however, presents a reversible negative interference by successfully competing with styrene for reaction with the trapping agent. The response to styrene exhibits a moderate positive humidity dependence. Following prolonged exposure, the original complex can be regenerated in situ by exposure to ethylene gas, permitting repeated use of the sensor. An emphasis is placed on the application of the sensor to workplace air monitoring.

### INTRODUCTION

Styrene is used principally for the industrial-scale production of polymer resins and thermoplastics, often in combination with other vinyl monomers such as acrylonitrile,

butadiene, or various acrylates (1). While industrial surveys have shown that exposure to these monomers during polymer production is minimized by the use of closed reactor systems, transient releases can occur during transfer to and from storage vessels and during maintenance operations (2). Subsequent processing of polymer materials can also result in exposure to residual monomers (3).

Exposure to styrene is also encountered in the fiber-reinforced plastics (FRP) industry (2). In a typical FRP operation, the viscous resin-laden fiber material is sprayed onto a product mold and then manually rolled out to remove entrapped air. The resin contains a high percentage of styrene, along with curing agents, binders and other volatile solvents that off-gas during this process. The most common air contaminants found in the FRP workplace along with styrene are aromatic hydrocarbons (e.g., ethylbenzene and toluene), chlorinated hydrocarbons (e.g., methylene chloride), and aliphatic ketones (e.g., acetone and 2-butanone) (2).

Occupational exposure to styrene vapor has been associated with impairment of the central and peripheral nervous systems as well as irritation of the eyes, skin, and upper respiratory tract (1, 2, 4). Styrene is also weakly mutagenic in vitro and in vivo (1, 5), presumably due to metabolic transformation to styrene 7,8-oxide followed by DNA alkylation (6). These data, coupled with findings of increased frequencies of chromosomal aberrations (7, 8) and sister chromatid exchanges (9) in the lymphocytes of styrene-exposed workers, suggest the possibility of styrene genotoxicity.

The recently revised Occupational Safety and Health Administration (OSHA) limits for styrene are 50 ppm based on an 8-h time weighted average (8-h TWA) and 100 ppm for short-term exposures (15-min TWA) (10). Similar workplace exposure limits are recommended by both the American Conference of Governmental Industrial Hygienists (ACGIH)

<sup>1</sup>Department of Environmental and Industrial Health, School of Public Health, University of Michigan.

<sup>2</sup>Department of Electrical Engineering and Computer Sciences and Berkeley Sensor and Actuator Center, University of California.

<sup>3</sup>Department of Biomedical and Environmental Health Sciences, School of Public Health, University of California.